OPTICAL REVIEW Vol. 20, No. 4 (2013) 338–340

Electro-Optical Detection of ZnO-Based Unbalanced Fabry–Perot Resonators

Feng ZHU, Yan-Hao YU, Ru-Long JIN, Ai-Wu LI*, Yong-Sen YU, and Han YANG†

State Key Laboratory on Integrated Optoelectronics, College of Electronic Science and Engineering, Jilin University, Changchun 130012, China

(Received September 4, 2012; revised April 17, 2013; Accepted May 30, 2013)

Zinc oxide films prepared by magnetron sputtering are introduced to the electro-optical detection to improve the voltage sensitivity. With the help of large piezoelectric effect, ZnO films make up for the deficiency of the low electro-optical coefficient. In this paper, we illustrated the mechanism of piezo-induced enhancements, and measured the electric signals on the line of coplanar waveguides. This method breaks through the limit of material species for optoelectronically responsive sensing, and shows promising applications in optical detection.

Keywords: electro-optical detection, electro-optic effect, the inverse piezoelectric effect, ZnO films, electric-field sensor

1. Introduction

Electro-optical detection, considered as a noninvasive electric-field measurement method, has attracted much attention, particularly in integrated-circuit (IC) fault diagnosis for probing the voltage characterization on internal lines or node of ICs.[1,2] The mechanism of this technique is the Pockels electro-optic effect, where the principle refractive indices of an electro-optical material (crystal or poled polymer) vary with the exciting electric field strength.[3,4] Due to the frequency-independence characteristic of the electro-optic effect, the electro-optical detection has a large bandwidth (DC to THz).[5,6] In IC detection, a piece of electro-optical material is usually sent in the fringing electric field of a measurement point of ICs. The surrounding optical system converts the phase modulation into intensity changes, when a laser beam travels through this sensing martial. Because the modulation is linearly proportional to the applied field strength, it is convenient to get the local electrical information of ICs. However, for electro-optic coefficients of the majority electro-optical materials are very small (usually only several pm/V),[7] this technology has intrinsically low voltage sensitivity which hampers its practical applications. Besides, the issue, associated with the low abrasive resistance of electro-optical crystals, makes it difficult to endure high-speed, multi-point, large area detection as an atomic force microscopic tip does.

In order to solve the problems mentioned above, zinc oxide (ZnO) films prepared by magnetron sputtering were introduced to this optical detection system. The phase retard of the probing beam ($\Delta\phi$) plays a critical role in this detection technique. Modulating effects to $\Delta\phi$ not only associate with the field-induced refractive index changes (Δn) by the electro-optic effect, but also thickness changes (Δd) by the inverse piezoelectric effect.[8,9] Although ZnO polycrystalline films have relatively lower electro-optic coefficient ($\gamma_{13} < 1$ pm/V), they have been extensively studied for its large piezoelectric tensors.[10,11] In this report, we use the piezoelectric contributions of ZnO films to enhance the voltage sensitivity of electro-optical detection system.[12] Additionally, ZnO films exhibit high performance on optical transparency, abrasion resistance, spontaneous preferred orientation of epitaxial growth and low substrate-dependence, which give a promising prospect in optical detection.

2. Principle

The schematic of the electro-optical detection system is shown in Fig. 1.[13,14] The light source is a continuous-wave laser diode of 1.31 μm wavelength. The monochromatic light rays are shaped into a parallel beam by ball lens, and we adjust the laser diode to guarantee light as much as possible pass through the polarizing beam splitter (PBS) vertically. Then, the output linear polarized beam is converted into circular polarized light by a $1/4\,\lambda$ plate, and it is directed to an objective lens, which focused the light, through an electro-optical probe, on the surface of the circuit under test. As the core element, the probe is made by first evaporating an aluminum (Al) thin film on the tip end of a glass cone, on which a polycrystalline film is sputtered for field sensing. The Al film serves as a high reflectance coating. The injected laser (I_{in}) passing through the probe is divided into two parts: one is reflected by the Al film as a reference beam (I_{ref}), and the other traveling through the ZnO film is reflected by the transmission line or node of ICs as a probing beam (I_{pro}). The electro-optic or piezoelectric effects of ZnO films cause a phase variation of I_{pro}, so the total reflected light intensity (I_R) carries the voltage information of the circuit under test. The reflected beam returns back to the PBS along the path it has come, and a part of the beam is reflected into the detector. Meanwhile, the circuit under test and the focused probing spot are monitored by a CCD camera and its illumination system. The field-induced changes of electro-optical materials thus are converted into detectable signals by an InGaAs infrared detector, and then these signals are amplified by a lock-in amplifier (EG&G 124A). Therefore, the internal electric information of ICs is acquired by monitoring the waveform's appearance on an oscilloscope.

As the detection configuration presented in the inset of Fig. 1, the probe and the circuit under test can be considered

*E-mail address: liaiwu2008@yahoo.com.cn
†E-mail address: hanyang@jlu.edu.cn

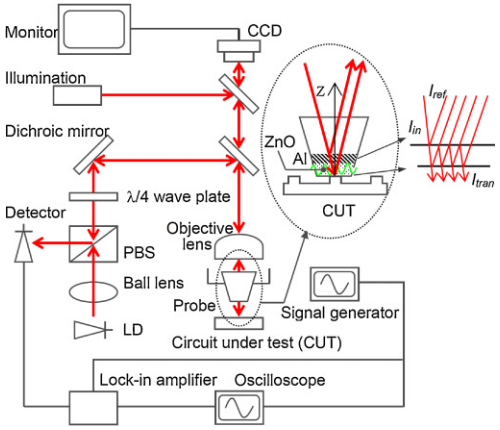

Fig. 1. (Color online) The schematic diagram of the electro-optical detection. The inset shows the probe configuration.

as an unbalanced Fabry–Perot resonator. The optical field of the reflected beam is described by the following equation:[15]

$$E_{\mathrm{R}} = -E_{\mathrm{in}} \cdot \frac{r_1 + r_2 e^{i\phi}}{1 + r_1 r_2 e^{-i\phi}}, \tag{1}$$

where E_{R} and E_{in} are the optical field amplitudes of the injected (I_{in}) and reflected (I_{R}) beam, r_1 and r_2 separately are the reflectance of the Al film and the circuit, and ϕ is the round-trip phase in the Fabry–Perot resonator. Different from conventional electro-optical detection, the piezoelectric effect of ZnO films is taken to enhance the filed modulation depth. Thus, the ϕ term not only depends on the refractive index variation of the material, but also the thickness change. In this case, the applied voltage is mainly longitudinal (z-direction of the inset of Fig. 1). According to the ∞ mm point group of ZnO polycrystalline films, we use the corresponding components: γ_{13} and d_{33}. If when sinusoidal voltage signals ($V_0 \sin \omega t$) are applied to the ZnO films, the round-trip phase would be expressed as

$$\begin{aligned} \phi &= \phi_0 + \Delta\phi = \phi_0 + \phi_{\mathrm{EO}} + \phi_{\mathrm{PZ}} \\ &= \frac{2\pi}{\lambda} 2n_0 d - \frac{2\pi}{\lambda} n_0^3 \gamma_{13} V_0 \sin(\omega t) \\ &\quad + \frac{2\pi}{\lambda} 2n_0 d_{33} V_0 \sin(\omega t), \end{aligned} \tag{2}$$

where ϕ_0 is the static round-trip phase, ϕ_{EO} and ϕ_{PE} are separately electro-optical and piezoelectric terms, d is the thickness of the material, γ_{13} is the electro-optical coefficient, and d_{33} is the piezoelectric constant. Taking these factors into account, the total reflected laser intensity can be described by

$$I_{\mathrm{R}} = E_{\mathrm{R}} \cdot E_{\mathrm{R}}^{*} = I_{\mathrm{in}} \frac{r_1^2 + r_2^2 + 2r_1 r_2 \cos\phi}{1 + r_1^2 r_2^2 + 2r_1 r_2 \cos\phi}, \tag{3}$$

where I_{in} is the intensity of the injected beam. Because the variations of ϕ are very small, the light intensity change caused by electric field can be written as

$$\begin{aligned} I_{\mathrm{EO}} = I_0 &\frac{4r_1 r_2 (1 - r_1^2)(1 - r_2^2) \sin\phi_0}{(1 + r_1^2 r_2^2 + 2r_1 r_2 \cos\phi_0)^2} \\ &\times \left(-\frac{2\pi}{\lambda} n_0^3 \gamma_{13} + \frac{2\pi}{\lambda} 2n_0 d_{33} \right) V_0 \sin(\omega t). \end{aligned} \tag{4}$$

Equation (4) shows electric signals are linearly converted into light-intensity signals. As we seen, the piezoelectric term enhance the modulation depth, because d_{33} is much larger than γ_{13} in ZnO crystals, especially ZnO polycrystalline films. It indicates that the piezoelectric effect can dramatically enhance the intrinsic sensitivity of the ZnO sensor. Besides, the voltage sensitivity is related to the reflectivity (r_1, r_2) and the static round-trip phase (ϕ_0). In order to further enhance the sensitivity, Al films thus are introduced to increase the reflectivity r_1 to 30–40%, and the resonator thickness is adjusted to satisfy the following equation: $\phi_0 \approx k\pi + \pi/2$ ($k = 0, 1, 2, \ldots$).

3. Experiments and Results

ZnO films with a well crystal orientation are important for electric field sensing. A detail study of ZnO films prepared by magnetron sputtering has been carried out by using X-ray diffraction (XRD). Prior to deposition, glass substrates were optically polished and treated with ultrasonic cleaning. Al films were epitaxially grown on the substrate by thermal evaporation. Subsequently, ZnO was deposited by magnetron sputtering with Ar as the sputtering gas mixed with O_2 as the reactive gas.[16] After deposition, these substrates were annealed with 600 °C for 30 min. The film quality is related to the sputtering condition: sputtering power, substrate temperature, the ratio of Ar and O_2. Experiments of exploring these grown conditions were carried out, and their crystal orientations were measured by XRD. These films have the c-axis perpendicular to the substrate. The full width at half maximum (FWHM) of the diffraction peak was used to identify the crystal quality. After careful experiments, we found ZnO films had excellent performances at the following preferred sputtering condition: sputtering power of 100 W, substrate temperature of 250 °C, the gas ratio of 2 : 1 (Ar : O_2). In that case, the sputtering rate was about 5 nm/min, and the film thickness could be controlled by the sputtering time. According to the resonance enhancement thickness from Eq. (4), we chose the thickness of about 660 nm to increase the modulation effect. Figure 2 shows the typical XRD pattern, and the FWHM is 0.26°.

According to the sputtering condition mentioned above, electro-optical probes based on ZnO films were fabricated. An aluminum film was first evaporated on the tip end of the fused silica cone of 200 μm diameter, and then a ZnO film of c-axis orientation was sputtered on it. As seen in Fig. 3, the ZnO film on the probe was confirmed by chemical component measurement. The inset of Fig. 3 shows the tip of the probe, and the rectangle range was the component measuring area.

In the electro-optical detection, the coplanar waveguides fabricated by photolithography were used to server as circuits under test as seen in the inset of Fig. 4(b). The lines of the coplanar waveguides are substituted for the transmission lines on the circuit surface: one is connected to the measured signal, and the other is grounded. The light spot on the line is the focused spot of the probe beam, the measurement point. Figure 4(a) is the typical data picked up in the lock-in amplifier, which shows the modulation signal

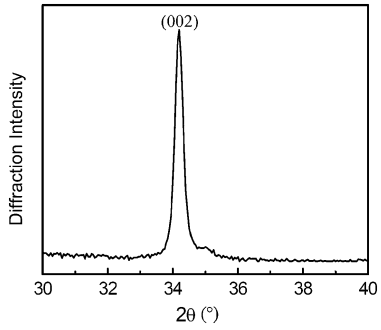

Fig. 2. XRD pattern of a *c*-axis oriented ZnO film on the glass substrate.

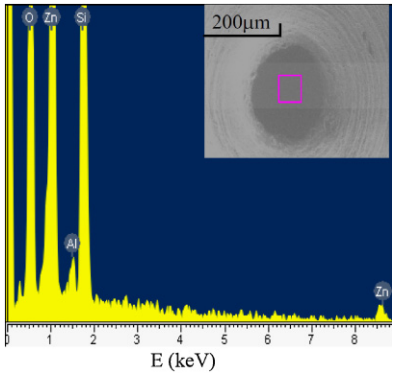

Fig. 3. (Color online) The chemical component measurement of the ZnO probe. The inset shows the tip end of the probe and the measuring area.

as a function of time when a sine wave with the amplitude of 10 V and the frequency of 1 kHz is applied to the signal line of the coplanar waveguide. For the ZnO probe, both the piezoelectric and electro-optic effects respond to the exciting electric field linearly. As a result, the picked signals were linearly dependent on the actually applied voltages with a coefficient determined by the optical system in Fig. 4(b), and the linearity was highly reproducible for different tips and different circuit samples.

4. Summary

In summary, ZnO films prepared by magnetron sputtering were introduced to enhance the voltage sensitivity of the electro-optical detection by its larger piezoelectric property. The cutoff frequency of the piezoelectric effect as an acoustic effect is usually in the order of MHz, much lower than that of the electro-optic effect which is nearly frequency independent. While piezoelectric effects may hinder a flat frequency response, in certain applications they could offer responsivities far greater than those offered by the electro-optic effect alone. However, although most of the typical ICs use broadband electronic signals from direct current to GHz, low-frequency or static test is irreplaceable in the integrated circuit fault diagnosis and design improvement domain. In addition, the light phase modulation induced by the acoustic effect expands material species for optically field sensing in the low-frequency range.[17–19)]

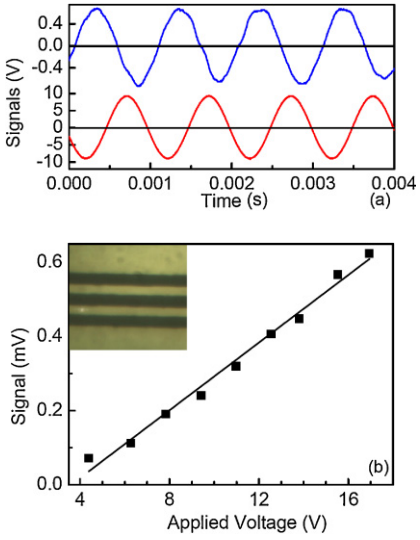

Fig. 4. (Color online) The electric-field measurement by using ZnO probes. (a) The upper curve shows the light intensity read by the photodiode detector, and the bottom curve is the applied electric signal to the line of the circuit. (b) The linear relation between the signals collected and the applied voltages. The inset is the coplanar waveguide served as a circuit under test, and the line width is 10 μm.

References

1) M. Shinagawa and T. Nagatsuma: IEEE Trans. Instrum. Meas. **43** (1994) 843.
2) L. Duvillaret, J.-M. Lourtioz, and L. Chusseau: Electron. Lett. **31** (1995) 23.
3) H. Cao, T. F. Heinz, and A. Nahata: Opt. Lett. **27** (2002) 775.
4) K. de Kort, A. Heringa, and J. J. Vrehen: J. Appl. Phys. **76** (1994) 1794.
5) Q. Wu and X.-C. Zhang: Appl. Phys. Lett. **68** (1996) 1604.
6) M. Shinagawa and T. Nagatsuma: IEEE Trans. Instrum. Meas. **41** (1992) 375.
7) O. Mitrofanov, A. Gasparyan, L. N. Pfeiffer, and K. W. West: Appl. Phys. Lett. **86** (2005) 202103.
8) R.-L. Jin, H. Yang, D. Zhao, Q.-D. Chen, Z.-X. Yan, M.-B. Yi, and H.-B. Sun: Opt. Lett. **35** (2010) 580.
9) W. Shi, Y. J. Ding, X. Mu, X. Yin, and C. Fang: Appl. Phys. Lett. **79** (2001) 3749.
10) A. Ashrafi and C. Jagadish: J. Appl. Phys. **102** (2007) 071101.
11) A. Ashida, T. Nagata, and N. Fujimura: J. Appl. Phys. **99** (2006) 013509.
12) A. Garzarella, S. B. Qadri, T. J. Wieting, and D. H. Wu: J. Appl. Phys. **98** (2005) 043113.
13) R.-L. Jin, H. Yang, Y.-H. Yu, D. Zhao, J. Yao, F. Zhu, Q.-D. Chen, M.-B. Yi, and H.-B. Sun: Opt. Lett. **36** (2011) 1158.
14) R.-L. Jin, H. Yang, D. Zhao, F. Zhu, Y.-H. Yu, Q.-D. Chen, M.-B. Yi, and H.-B. Sun: IEEE Photonics J. **3** (2011) 57.
15) P. O. Muller, D. Erasme, and B. Huyart: IEEE Trans. Microwave Theory Tech. **47** (1999) 308.
16) X.-B. Li, S. Limpijumnong, W. Q. Tian, H.-B. Sun, and S. B. Zhang: Phys. Rev. B **78** (2008) 113203.
17) X. Cheng, J. Zhang, T. Ding, Z. Wei, H. Li, and Z. Wang: Light Sci. Appl. **2** (2013) e80.
18) R.-L. Jin, Y.-H. Yu, H. Yang, F. Zhu, Q.-D. Chen, M.-B. Yi, and H.-B. Sun: IEEE J. Quantum Electron **48** (2012) 1310.
19) D. Lepage, A. Jiménez, J. Beauvais, and J. J. Dubowski: Light Sci. Appl. **2** (2013) e62.